Materials Chemistry and Physics 212 (2018) 113–121

Contents lists available at ScienceDirect

Materials Chemistry and Physics

journal homepage: www.elsevier.com/locate/matchemphys

Structural evolution during the catalytic graphitization of a thermosetting refractory binder and oxidation resistance of the derived carbons

Segun I. Talabi [a, b, *], Ana P. Luz [a], Victor C. Pandolfelli [a], Alessandra A. Lucas [a]

[a] Federal University of São Carlos, Materials Engineering Department, Rod. Washington Luiz, km 235, São Carlos, SP, 13565-905, Brazil
[b] University of Ilorin, Materials and Metallurgical Engineering Department, PMB 1515, Ilorin, Kwara State, Nigeria

HIGHLIGHTS

- Structural evolution during pyrolysis of novolac resin containing H_3BO_3 or B_2O_3.
- The catalytic graphitization depends on B–*O*–C formation and cleavage.
- Composition, bond strength and crystallization controlled the carbons' reactivity.
- Better oxidation resistance can be attained without the carbon's crystallization.

ARTICLE INFO

Article history:
Available online 13 March 2018

Keywords:
Graphitization
Novolac resin
Structural evolution
Oxidation resistance

ABSTRACT

Carbon-containing refractories' (CCRs) thermomechanical properties depend on the presence of carbonaceous phase with a structure and features similar to those of graphite. Based on this, boron oxide and boric acid were used to induce graphite generation during the pyrolysis of novolac resin (binder for CCRs) to provide an additional source of crystalline carbons. In this study, the structural evolution leading to crystallization of the derived carbons was studied via Fourier Transform Infrared (FTIR) spectroscopy. The results showed that the carbons graphitization was as a result of the formation and cleavage of the B–*O*–C bond during heat treatment. The lower binding energy of this bond compared to plain C–C bond permits carbon atoms rotation and restructuring necessary for graphite generation during the pyrolysis operation. Furthermore, the research investigated the oxidation resistance of the derived carbon samples with the aid of thermogravimetric (TGA) and differential scanning calorimetry (DSC) equipment. The influence of different mixing routes at the preparation stage and hexamethylenetetramine (HMTA) addition to the resin formulations on the carbons' oxidation resistance was also examined. The analysis provides insight on the parameters that control the oxidizing behavior of the different samples obtained based on these variations. Several factors including graphitization, composition and atoms bond strength were observed to influence their performance when the carbons were exposed to the non-reducing environment at high temperatures up to 1000 °C.

1. Introduction

Carbon-containing refractories' (CCRs) thermomechanical performances are significantly influenced by the added graphite and binder component [1,2]. The carbonaceous phase acts as a non-wetting material, which minimizes slag penetration into the brick during steel-making applications [3]. The polymer products used to link the coarse and fine refractory particles together provides green mechanical strength, reduce porosity, and acts as an additional carbon source.

Due to environmental concerns, thermosetting resins (novolac, resole) have replaced the conventional binders such as coal tar or pitch, which produces graphitizable carbon with superior oxidation resistance. Phenolic resins emit minimal polycyclic aromatic hydrocarbons and other toxic substances during their pyrolysis and therefore provide greater health benefits [4,5]. Unlike pitch-bonded

* Corresponding author. Federal University of São Carlos, Materials Engineering Department,Rod. Washington Luiz, km 235, São Carlos, SP, 13565-905, Brazil.
E-mail address: talabi.si@unilorin.edu.ng (S.I. Talabi).

https://doi.org/10.1016/j.matchemphys.2018.03.029
0254-0584/

bricks, which show expansion after tempering, resin-bonded ones exhibit lesser shrinkage irrespective of the carbon content and their usage (thermosetting resins) offers the advantage of cold-mixing [2]. Nevertheless, the significance of carbon derived from these resins is still limited because they possess poor oxidation resistance (because of their isotropic nature) and cannot compensate for excess stresses (except by microcracks formation) due to their hardness and brittleness [1]. These types of organic precursors do not undergo reconstructive transformation during heating in an inert environment because their pyrolysis is exclusively a solid state reaction, which occurs without the formation of liquid or semi-liquid components.

Carbons' oxidation resistance depends on their accessibility by the reacting media and bond strength between their atoms. Their composition and atomic arrangement also influence this property. Crystalline carbons have improved oxidation resistance than the amorphous or glassy ones [6] due to the reduced amount of edge site atoms and their anisotropic nature [7–9]. Therefore, graphite's generation during pyrolysis of non-graphitizable organic precursors such as thermosetting resins should reduce the resulting carbons' reactivity in oxygen.

Moreover, the depletion rate of carbon in CCRs will determine their service life and performance consistency in terms of thermal shock resistance and infiltration. Consequently, there is an increasing interest to achieve the graphitization of phenolic resin carbons using processing parameters that can be adopted for the production of CCRs. The use of certain additives has been reported to induce crystallization of phenolic resin carbons through a process referred to as catalytic graphitization [10–12]. The results obtained from such studies confirmed an improvement in the oxidation resistance of the derived carbons [13,14]. In additions to this benefit, the CCRs developed based on in-situ graphitization of the thermosetting resin component have improved mechanical properties [1,15].

The catalytic graphitization of novolac resin containing either boric acid or boron oxide was reported by Talabi et al. [16]. The research focused on the role that some processing parameters such as mixing technique, heat treatment procedure and heating rate have on the amount of generated crystalline carbons. However, the reaction that led to graphite generation during the modified-resin carbonization was not analyzed. Consequently, this study investigates and discusses the structural evolution that occurs during the thermal treatment of the H_3BO_3 and B_2O_3-modified novolac resin and provided insight on the mechanism leading to their graphitization. Furthermore, the oxidation stability of the resulting carbon was studied with the aid of thermogravimetric (TGA) and differential scanning calorimetry (DSC) equipment. The carbons reactivity in an oxidizing environment and the attained graphitization level were compared to ascertain the relationship between both parameters.

2. Experimental procedures

Novolac resin (Nv) was selected for investigation as an additional source of crystalline carbons in carbon-containing refractories. Firstly, a reference sample was prepared from a mixture of novolac resin and 10 wt% hexamethylenetetramine (HMTA, $d < 200\ \mu m$). Thereafter, commercial novolac resin (Nv) was mixed with either 6 wt% boron oxide or 10 wt% boric acid (the graphitizing agents). The weight percentages of H_3BO_3 and B_2O_3 in the formulation are equivalent. Also, the effect of HMTA incorporation into the modified resin was investigated. The formulations' components were mixed primarily with the aid of a mechanical mixer at 30 rpm for 20 min for homogeneous dispersion of the additives within the resin. The effect of additional ultrasonic mixing (for 15 min) or vacuum degassing (for 10 min) during the preparation stage on oxidation resistance of the derived carbons were also studied. These procedures were incorporated to facilitate proper dispersion of the additives and remove oxygen introduced during mechanical mixing respectively. Each of the prepared compositions was poured into an alumina crucible, covered with disk and embedded in a refractory box filled with coke to create a reducing environment during the step-wise pyrolysis procedure. The process involved heating the samples to 100 °C with a hold time of 4 h before raising the temperature to 500 °C with a hold time of 1 h and then to 1000 °C and keeping it at that temperature for 5 h. The heating rate of 3 °C/min was employed for the entire heating steps. The raw materials information with samples and preparation designations, were presented in Table 1. The B and H represent B_2O_3 and H_3BO_3 respectively. The number by the side of the different additives stands for their percentage weight in the formulation (e.g., 6B stands for 6 wt% B_2O_3). The letter “M” in the sample designation stands for “mechanical mixing,” the “U” represents “additional ultrasonic mixing” and “V” stands for “additional vacuum degassing.”

After carbonization, the samples were cooled to room temperature inside the muffle furnace at a cooling rate of ~16 °C/min and ground in an AMEF vibratory disc mill for 12s. A NETZSCH STA 449F3 (Netzsch Inc., Germany)-type thermogravimetric (TGA) and differential scanning calorimetry (DSC) analyzer was used to determine the samples' behavior in an oxidizing environment. The apparatus detects mass loss and heat flow with a resolution of 0.001 g and 0.00001 mW/mg respectively, as a function of temperature and time. Before carrying out the test, the samples were evenly distributed in an alumina sample pan. The analysis was performed in synthetic air (80% N_2, 20% O_2) at 50 cm^3/min flow rate starting from 30 °C to 1000°C ± 10 °C with 10°C/min heating rate. Due to the presence of impurities, the thermogravimetric (TG) curves were normalized to eliminate the contribution of the non-carbon material. Firstly, the inflection point temperature, which represents the onset of carbons oxidation was determined from the non-isothermal TG curves as depicted in Fig. 1. The final residual mass (RM_f) was then subtracted from the one at the onset of carbon oxidation (MO_i) to obtain the actual carbon loss (x). Subsequently, the actual residual mass of carbons at the end of the measurement (RM_a) was calculated according to equation 1.

$$RM_a = 100 - \left(MO_i - RM_f\right) \quad (1)$$

RM_a was used to describe the overall oxidation resistance of the pyrolytic carbons. Moreover, the information from the DSC curves was used to complement the deductions from the TG curves and FTIR spectra.

Fourier Transform Infrared (FTIR) spectroscopy was used to study the structural evolution that occurs during thermal cross-linking (100 °C/4h + 230 °C/1h), carbonization (100 °C/4h + 230 °C/1h + 500 °C/1h) and graphitization (100 °C/4h + 230 °C/1h + 500 °C/1h + 1000 °C/5h) stages. The FTIR spectra were recorded via a Varian 640-IR spectrometer between 400 and 4000 cm^{-1}, 64 accumulations, and 4 cm^{-1} resolution using the standard KBr method. For this analysis, each sample and KBr powder were dried in an oven at 110 °C for 24 h to remove moisture. 200 mg of fine KBr was mixed with 2 mg of the carbon samples, pulverized and then pressed to form transparent pellets that were used for the characterization.

Table 1
General information about raw materials with samples and process designations.

Raw Materials	Main Features	Supplier
Novolac resin	Nv, Prefere® 88 5010R, Liquid (solvent = ethylene glycol) Density = 1.18 g/cm^3	Dynea, Brazil
Boric acid	H_3BO_3, solid powder, $d_{90} < 45$ μm, 99%	Synth Chemical Co., SP-Brazil
Boron oxide	B_2O_3, solid powder, $d_{50} < 10$ μm, 99% purity	Magnesita Refratários, SA
Hexamethylenetetramine	HMTA, d < 200 μm	Dynea, Brazil
Samples Designation		
Nv-HMTA (reference sample)	Nv+10 wt% HMTA	
Nv-6B	Nv + 6 wt% B_2O_3	
Nv-10H	Nv + 10 wt% H_3BO_3	
Nv-HMTA-6B	Nv + 10 wt% HMTA + 6 wt% B_2O_3	
Nv-HMTA-10H	Nv + 10 wt% HMTA + 10 wt% H_3BO_3	
Preparation Designation		
M	Mechanical mixing	
M-U	Mechanical mixing + Ultrasonic mixing	
M-V	Mechanical mixing + Vacuum degassing	

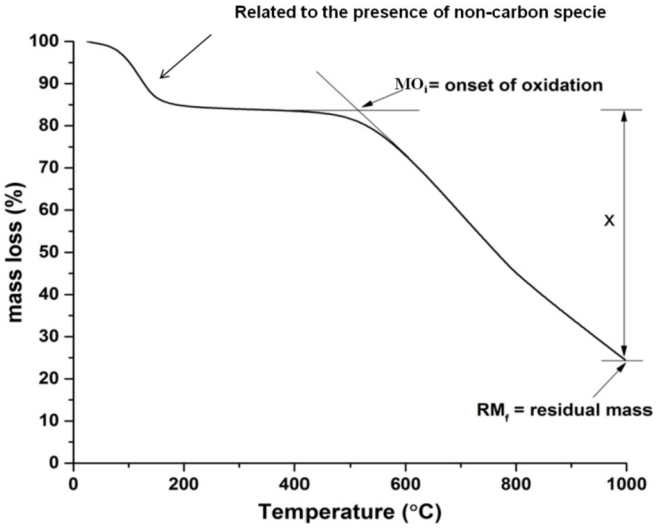

Fig. 1. Curve showing parameters used to determine the actual carbon loss.

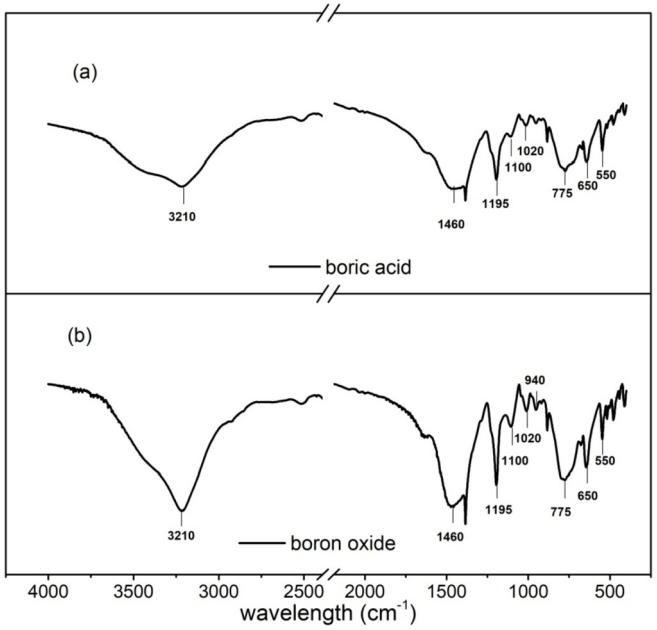

Fig. 2. FTIR spectra of the graphitizing agents: (a) boric acid (b) boron oxide.

3. Results and discussion

3.1. FTIR spectra of the graphitizing agents

Fig. 2 represents the spectra contours of the boron compound additives (i.e., H_3BO_3 and B_2O_3). As a result of hydrogen atoms orientation relative to the $B_3O_3(O^-)_3$ backbone, boric acid has low symmetry [17]. Its molecules can be classified into the motions of the hydrogen atoms and $B_3O_3(O^-)_3$ skeleton [17,18]. Many broad bands, which correspond to different structure-forming OH groups characterized boric acid spectrum [18]. The strong band at 650 cm^{-1}, 1195 cm^{-1}, and 1460 cm^{-1} are found in boric acid [19]. The band at 650 cm^{-1} was due to the deformation vibrations of the B—O bond atoms. According to Medvedev et al. [19], the weak band at ~940 cm may be due to the presence of metaboric acid. The band at 1020 cm^{-1} indicates the presence of structuring-forming [BO_4] groups [19,20]. The peak at 1390 cm^{-1} was due to the vibration of in the B(3)-O$^-$ bond in [BO_3] or $B_3^{10}O_3(OH)_3$ groups [19]. The band at 1632 cm^{-1} corresponds to water molecule vibration. When boron oxide spectrum was superimposed on boric acid, similar peaks were present. The only identified difference was in their bands' area and intensity. For example, the spectrum peak area at ~3200 cm^{-1} belonging to the OH group of boron oxide was higher than that of boric acid, which may be due to its higher hygroscopic characteristic compared to boric acid.

3.2. FTIR spectra of the plain and cured novolac resin

The characteristic bands detected in plain novolac resin were assigned based on literature review and IR spectra database as shown in Table 2. As expected, the peaks assigned to the various chemical groups varied slightly in the literature. The spectra in the wavelength range from 400 to 4000 cm^{-1} are shown in Fig. 3. The peaks at 755 cm^{-1}, 815 cm^{-1}, and 890 cm^{-1} correspond to C—H vibrations while the ones at 1050 cm^{-1} and 1064 cm^{-1} correspond to the C—O stretching vibrations of CH_2OH group. The bands, which correspond to C—*O*—C aliphatic ether and an asymmetric stretch of phenol were detected at 1125 cm^{-1} and 1230 cm^{-1} respectively. The width of the band at 1355 cm^{-1} and 3300 cm^{-1} indicated that these peaks were due to O—H bond vibration. Additional peaks, which correspond to C=C aromatic ring vibration were detected at 1510, 1595 and 1645 cm^{-1} wavenumber. The one at 2929 cm^{-1} corresponds to aliphatic -CH_2 in-phase stretch.

It can be seen from Fig. 3a that the band belonging to phenolic hydroxyl group vibration in the plain resin at 3300 cm^{-1} and mostly all the other peaks became weaker with increased heat treatment temperature up to 230 °C/1h. However, no new peak was

Table 2
IR bands detected in the plain and cured novolac resin.

Peaks (cm^{-1})	Functional group	Reference
3300	Phenolic −OH stretch	Liu 2002 et al. [24], Ida et al. [25]
2929	Aliphatic -CH_2 in-phase stretch	Theodoropoulou et al. [26], Ida et al. [25], Ertugrul et al. [27]
2865	Out of phase stretching of CH_2	Ida et al. [25]
1645	C=C stretching vibration of aromatic ring	Wang et al. [28], Theodoropoulou et al. [26]
1595	C=C stretching vibration of aromatic ring	Ida et al. [25]
1510	C=C aromatic ring	Ida et al. [25]
1440	C=C benzene ring obscured by -CH_2- methylene bridge	Ida et al. [25]
1355	OH in-plane	Ida et al. [25]
1230	the asymmetric stretch of phenolic C−C−OH	Wang et al. [28], Kawamoto et al. [29], Wang et al. [30] http://webbook.nist.gov, Ida et al. [25]
1125	stretching vibration of C−*O*−C aliphatic ether	Ida et al. [25], Theodoropoulou et al. [26], Ertugrul et al. [27]
1064	C−O stretching vibrations of CH_2OH group	Liu et al. [24], Ida et al. [25]
1050	C−O stretching vibrations of CH_2OH group	Liu et al. [24], Ida et al. [25]
890	CH out-of-plane, isolated H	Ida et al. [25]
815	CH out-of-plane, substituted	Ertugrul et al. [27], Theodoropoulou et al. [26], Ida et al. [25]
755	CH out of plane, ortho-substituted	Ida et al. [25]

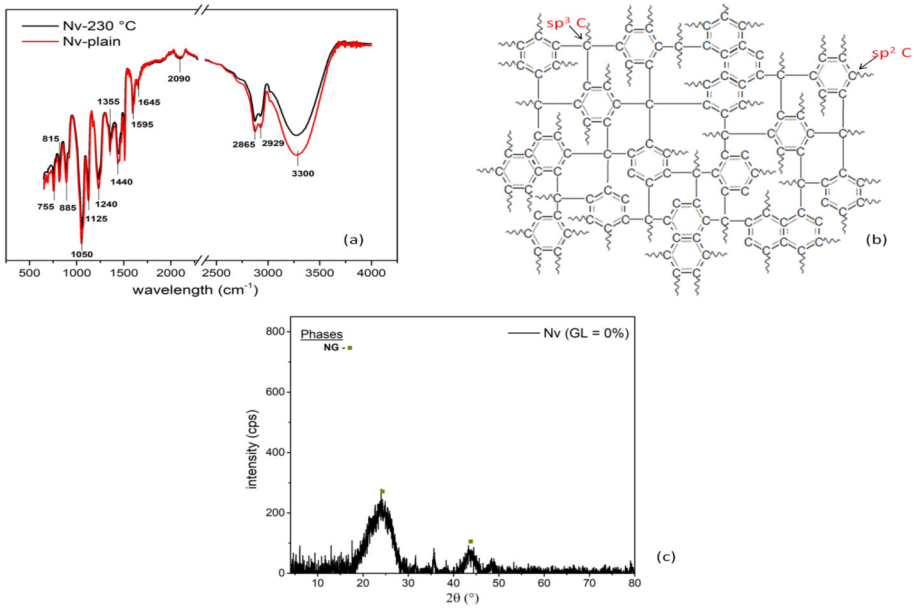

Fig. 3. (a) FTIR spectra of plain and cured novolac resin at 230 °C, (b) schematic structure of fully carbonized phenolic resin [23], (c) X-ray diffraction pattern of carbon derived from the plain novolac resin at 1000 °C/5h.

found at 230 °C. This type of structural evolution suggests that decomposition and thermal cross-linking process led to char formation [21,22]. The thermal degradation process resulting in the production of glassy/non-graphitic carbon may proceed according to the order proposed by Lee [23]. This process starts by bond breaking reactions, forming free radicals and depend on the dissociating energy of radicals present in the resin (i.e., the stability of free radical = ease of formation = triphenylmethyl > diphenylmethyl > benzyl > phenoxy > alkyl > phenyl). Typically, glassy carbons derived from plain novolac resin consist of 6 member sp^2 bonded cyclic structures, which are held tightly within a network of sp^3 crosslink [23] that does not permit reorganization or rotation necessary for graphitization (Fig. 3b). Both inert pyrolysis and to a limited extent oxidation/combustion coexist during the thermal decomposition process due to the presence of reaction water, absorbed moisture and hydroxyl groups in the resin's structure [23]. Nevertheless, the oxidation reaction is limited to the effect of generated oxygen radicals on their way out of the polymer sites during the inert pyrolytic decomposition. The diffraction pattern of the resulting glassy carbon was presented in Fig. 3c.

HMTA is usually added to novolac resin for use as a binder during the industrial preparation of carbon-containing refractories. Based on this information, a reference composition containing 10 wt% HMTA (Nv-HMTA) was heat treated up to 230 °C/1h. The spectrum of the cured reference novolac resin was presented in Fig. 4a. Although no new functional group (compared to the plain novolac sample) was detected, some minor peaks shift occurred. Fig. 4b shows the diffraction pattern of the derived carbon, which is typical of sp^3-hybridized carbons with an amorphous structural arrangement due to the atoms limited rotation during carbonization [16].

3.3. Structural evolution during pyrolysis of the modified resin

The peaks detected in the novolac resin containing the boron source additives were assigned as shown in Table 3. The structural evolution that occurs when Nv-10H formulation (novolac resin +10 wt% boric acid) was subjected to thermal treatment up to 230 °C, 500 °C and 1000 °C was represented by the spectra in

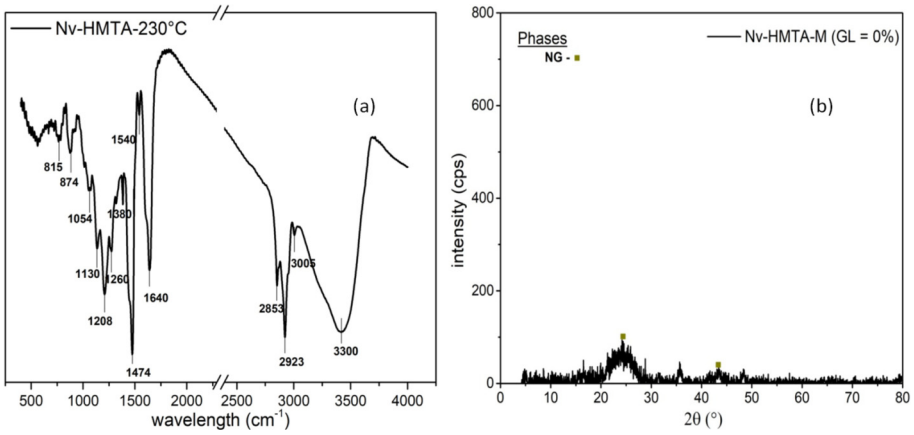

Fig. 4. (a) Novolac resin +10 wt% HMTA (reference composition) heat treated up to 230 °C, (b) X-ray diffraction pattern of reference composition after firing up to 1000 °C and a hold time of 5h. GL = graphitization level, NG = non-graphitic.

Fig. 5a.

Compared to the unmodified cured resin some new bands were detected at 885 cm^{-1} and 1440 cm^{-1}, which correspond to B–O vibration attributed to phenyl borate formation as shown in Fig. 5b [28,30]. The peak intensity at 885 cm^{-1} decreased with increasing treatment temperature (it was still detected at 500 °C) and disappeared at 1000 °C. This observation suggested that B–*O*–B formation and dissociation was gradual and is a function of increasing temperature [31]. According to Ertugrul et al. [27], this reaction depends on the production route and time. Furthermore, the presence of the bond ascribed to phenyl borate formation indicates that chemical reaction between the additive and resin occurs at an early stage (230 °C). Wang et al. [28], observed that higher temperature up to 200 °C was required to initiate a reaction between B–OH and phenolic hydroxyl group to form phenyl borate. Similarly, Liu et al. [24] attributed borate formation to the reaction of phenol and benzyl hydroxyl groups with boric acid. Furthermore, the band assigned to the stretching vibration of B–*O*–C group appears at ~1320 cm^{-1} after thermal treatment up to 500 °C. This peak was not detected at 230 °C and after the pyrolysis process at 1000 °C. The transition of the B–*O*–C supports the assertion that its formation and cleavage plays a significant role in the catalytic graphitization of novolac resin containing boron based additives [16,28]. The weakest bond in the polymer chain (at this instance, B–*O*–C) led to chain cleavage, which permits the disruption and structuring during pyrolysis that favors graphite generation at a lower temperature such as 1000 °C (as seen by the sharpness and intensity of the peak at 26° in Fig. 5c). Based on the XRD profile analysis, a graphitization level of 69% was attained. The amount of crystalline carbon was calculated according to the description of Bitencourt et al. [11]. However, the generation of graphite during pyrolysis may be heterogeneous in nature due to preferential graphitization starting from low energy binding sites [16]. The spectra analysis further justifies this assertion as the B–*O*–C bond has lesser binding energy (190.2 eV [28]) compared to plain C–C (284.8 eV) ones, which characterized the uncatalyzed resin. Moreover, the cleavage of this bond can lead to boron introduction into the carbon's structure. Boron atoms due to their enhanced diffusivity can intercalate carbon atoms during the pyrolysis and about change in π-electron density and reduced interlayer spacing [32,33].

Furthermore, the medium bands intensities between 1617 and 1647 cm^{-1} were assigned to C=C vibration stretching of the aromatic ring [24,27]. As the process proceeds, phenol hydroxyl and benzyl hydroxyl absorption bands decreased due to borate formation and water evolution [28] as observed by the decrease in the –OH band percentage area with increasing heat treatment temperature. This consideration agrees with Jiang et al. [34] and Wang et al. [28] submission that water evolution and additional intermolecular cross-linking occurs at the early stages of pyrolysis. The produced water can also be attributed to cleavage of the hydroxyl link and the reaction between B–OH and phenolic hydroxyl groups

Table 3
FTIR spectra of novolac resin containing boron source additives heat treated up to 230 °C, 500 °C, and 1000 °C.

Peaks (cm^{-1})	Functional group	Reference
3350–3400	Phenolic –OH stretch	Liu 2002 et al. [24], Ida et al. [25]
2925	Aliphatic -CH_2 in-phase stretch	Theodoropoulou et al. [26], Ida et al. [25], Ertugrul et al. [27]
1890, 875	B–O bond	Medvedev et al. [19], Ertugrul et al. [27], http://webbook.nist.gov
1600–1650	C=C stretching vibration of aromatic ring	Wang et al. [28], Theodoropoulou et al. [26]
1510–1550	C=C aromatic ring	Ida et al. [25]
1430	B–*O*–B	Liu et al. [24], Wang et al. [28], http://webbook.nist.gov
1380	OH in-plane	Ida et al. [25]
1310–1350	B–*O*–C	Wang et al. [28], http://webbook.nist.gov
1222	the asymmetric stretch of phenolic C–C–OH	Wang et al. [28], Li et al., Kawamoto et al. [29], Wang et al. [30] http://webbook.nist.gov, Ida et al. [25]
1120–1125	stretching vibration of C–O–C aliphatic ether	Ida et al. [25], Theodoropoulou et al. [26], Ertugrul et al. [27]
1050	single bond C–O stretching vibrations of CH_2OH group	Liu et al. [24], Ida et al. [25]
815	CH out-of-plane, substituted	Ertugrul et al. [27], Theodoropoulou et al. [26], Ida et al. [25]
775	B–O bond belonging to boron source additives	
≤750	CH out-of-plane, substituted, ortho-substituted	Ertugrul et al. [27], Theodoropoulou et al. [26], Ida et al. [25]

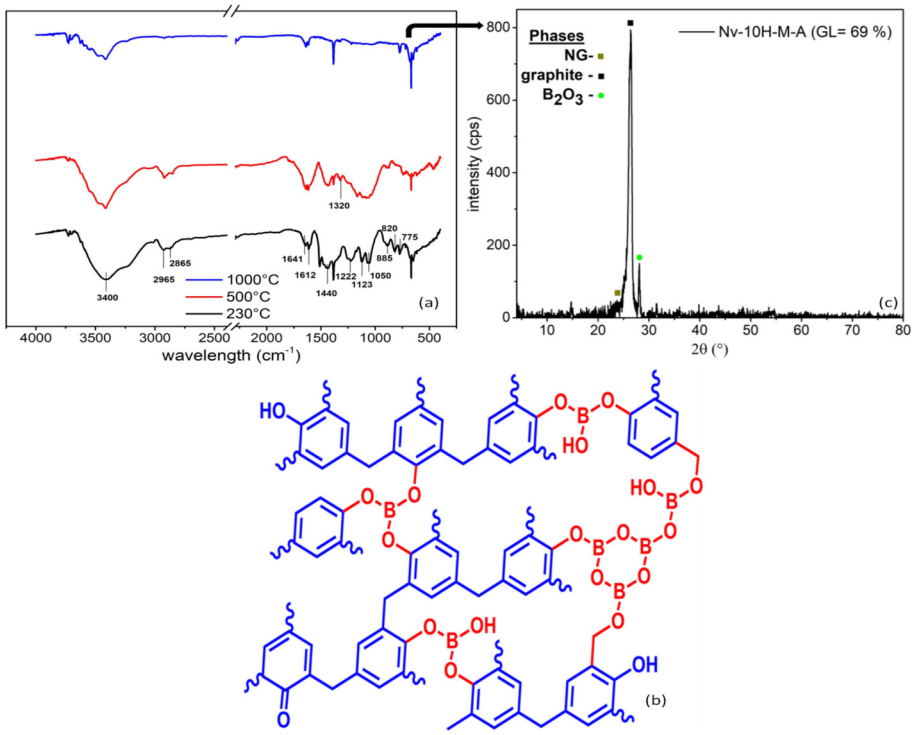

Fig. 5. (a) FTIR spectra of novolac resin composition containing 10 wt% boric acid, heated up to 230 °C/1h, 500 °C/1h and 1000 °C/5h, (b) Structural representation of cured boric acid modified novolac resin [28], (c) XRD diffraction pattern of carbon derived from novolac resin containing 10 wt% boric acid. GL = graphitization level, NG = non-graphitic.

[23,28]. The decrease with the firing temperature in the intensities of multiple absorption peaks at 820 cm^{-1} corresponding to C–H flexural vibration of benzene ring shows that the volatilization of methyl and phenol derivatives occurs and that dehydrogenation and carbonization reaction were more pronounced above 500 °C.

The spectra showing structural evolution during pyrolysis of boron oxide modified resin are shown in Fig. 6a. The structural representation and diffractogram of the derived carbon were

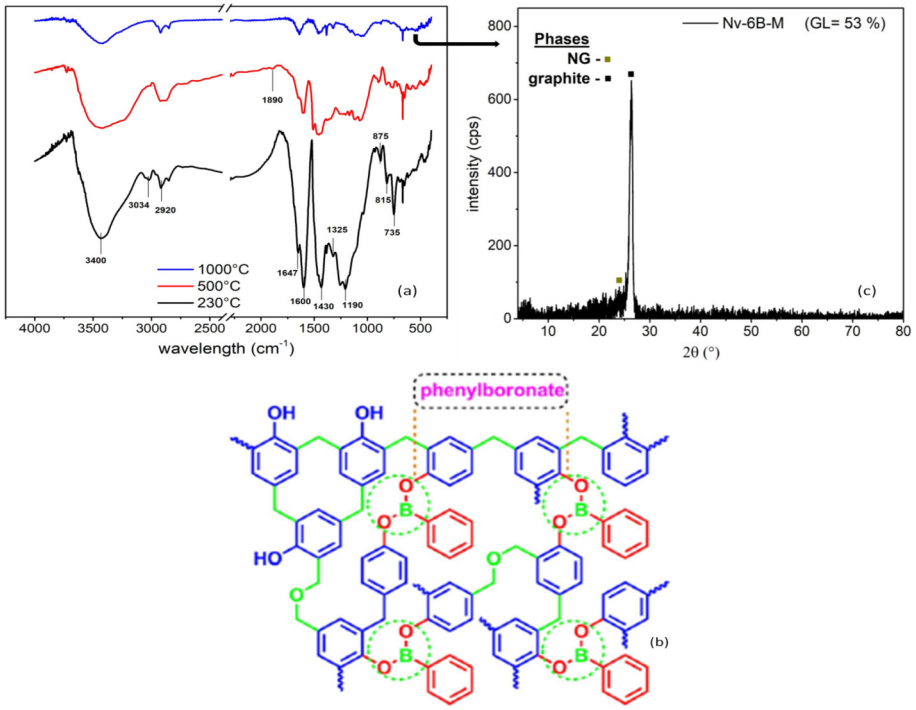

Fig. 6. (a) FTIR spectra of novolac resin composition containing 6 wt% boron oxide heat treated up to 230 °C/1h, 500 °C/1h and 1000 °C/5h (b) Structural representation of cured boron oxide modified novolac resin [30], (c) XRD diffraction pattern of carbon derived from novolac resin containing 6 wt% boron oxide. GL = graphitization level, NG = non-graphitic.

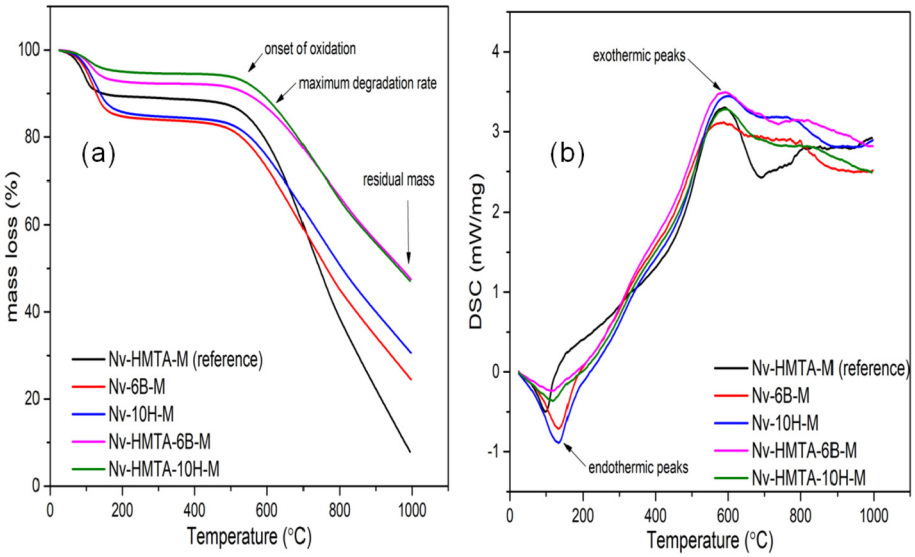

Fig. 7. (a) Descriptive TG curves (b) Descriptive DSC curves of carbons derived boron catalyzed novolac resin.

presented in Fig. 6b and c respectively. At this instance, B—*O*—C bond (1330 cm^{-1}) was detected earlier at 230 °C. The likely reasons for this change may be due to boron oxide smaller particles size ($d_{50} < 10$ μm) compared to boric acid ($d_{50} < 45$ μm), which promoted a more rapid reaction. The band due to phenyl borate formation was detected at 1430 cm^{-1}.

3.4. Oxidation resistance of carbons derived from novolac resin containing boron compounds additives

Fig. 7a typified the oxidation behavior of carbons derived from the novolac resin (reference) and the modified catalyzed resins evaluated in the present study. Firstly, the TG curves indicate the presence of non-carbon materials in the samples' composition (as seen by the initial mass loss between ~50 and 150 °C). This observation was confirmed by the endothermic region in the DSC curves within that same temperature range (Fig. 7b). Additionally, the FTIR analysis of the carbon samples confirms the presence of -OH functional group, which may be responsible for such behavior (Figs. 5a and 6a). This observation agrees with findings from the literature that significant amount of oxygen, carbon oxides and other impurities are present after pyrolysis of phenolic resins containing additives at 1000 °C [28,35,36]. For example, carbons derived from the pyrolysis of boric acid modified novolac resin at 1000 °C was reported to contain about 7% oxygen by Wang et al. [28]. However, all non-carbon species will be removed with increased carbonization temperature [19]. More so, the amount of the non-carbon material per sample was observed not to be the same for all the analyzed carbon samples (based on the TG curves). The observation may not be unconnected with the difference in the starting components of the resin formulation. Consequently, to enable proper estimation of carbon loss, the TG-curves were normalized and the actual residual mass was determined from the carbons' oxidation initiation point as explained in "Section 2". The data presented in Table 4 represent the average values of three analyses carried out on the same sample batch. Based on the attained results, the oxidation rate of the different carbon samples was found to differ as a function of the starting resin formulations. Compared to Nv-HMTA-M (26%), the residual mass of Nv-6B-M and Nv-10H-M carbons increased to an average value of 50 ± 5% and 52 ± 3% respectively. These values indicate a significant improvement in the oxidation resistance of the graphitized carbons. The chemical and structural properties of plain novolac resin compel it to yield glassy carbon during carbonization. Due to their isotropic structure, these types of carbons are more susceptible to oxidation. However, the structuring that took place during pyrolysis of the

Table 4
Effect of graphitization, increased addition of HMTA and preparation procedure on the carbons' oxidation resistance.

Sample	RM_a (%)	Onset of Oxidation (T_i)	GL(%) [16]
Nv-HMTA-M	26	582	0
Nv-6B-M	50 ± 5	525 ± 12	47 ± 12
Nv-10H-M	52 ± 3	535 ± 12	49 ± 12
Nv-10HMTA-6B-M	54 ± 4	574 ± 4	0
Nv-10HMTA-10H-M	60 ± 3	566 ± 6	0
Nv-11HMTA-10H-M	60	573	0
Nv-12HMTA-10H-M	65	572	0
Nv-13HMTA-10H-M	64	572	0
Preparation procedure: Ultrasonic mixing incorporation			
Nv-6B-*M*-U	51	543	26
Nv-10H-*M*-U	53	540	13
Preparation procedure: Vacuum degassing incorporation			
Nv-6B-*M*-V	49	533	28
Nv-10H-*M*-V	50	527	7
GL – Graphitization level			

modified resin led to a reduction in the amount of edge site carbon atoms (which are more reactive than those of basal plane), reduced interlayer spacing and induced anisotropic characteristic which was beneficial for improved oxidation resistance [7–9]. Moreover, the rate controlling-step during high-temperature oxidation of carbon is believed to depend on oxygen transport through the solid boundary layer [37]. Apart from these, the presence of B_2O_3 detected in the sample's composition (Fig. 5c) will also protect the graphite microcrystallites edges during oxidation [38]. Therefore, the attained oxidation stability may be attributed to the formation of a protective coating on the carbon surface in addition to graphitization. Nevertheless, carbons derived from the boron compounds modified resin containing 10 wt% HMTA (especially for the formulation containing boric acid) show greater oxidation stability although graphite was not detected in their composition [16]. According to Edward et al. [39], the macromolecular (polymeric) structure of non-graphitizing materials remains during heat treatment, losing only small molecules by degradation and developing even more cross-linking during pyrolysis. Invariably, increased bond strength and presence of inclusion that can acts as a protective oxide in addition to minimal restructuring can result in higher oxidation resistance. The results obtained regarding this formulations show that optimal cross-linking of the novolac resin during the curing stage and the presence of boron oxide in the amorphous carbon can also improve carbons' oxidation stability [40,41].

To ascertain these deductions, more HMTA (11–13 wt%) was added to the boron compounds modified resin. The results further show that:

1. The increased amount of HMTA in the starting formulation of the modified resin can reduce their reactivity in air and that the oxidation of such carbons is not just a function of crystallization.
2. The presence of HMTA also plays a significant role on the oxidation onset temperature. Carbons derived from the compositions containing the cross-linking agent have higher T_i values. For example, the T_i for Nv + HMTA (reference) was 582 °C (the highest recorded value for all the investigated composition) compared to 535 °C of Nv-10H-M. Nevertheless, the overall performance of carbons derived from this formulation further indicated that other factors including graphitization and composition affect their oxidation process.

Regarding Nv-6B-*M*-U, Nv-10H-*M*-U, Nv-6B-*M*-V and Nv-10H-*M*-V carbons, the introduction of either additional ultrasonic mixing or vacuum degassing after the initial mechanical mixing led to significant reduction in the generated amount of graphite after pyrolysis (Fig. 8, Table 4). The additional mixing technique induces high energy chemical reactions due to the formation, growth, and collapse of bubbles, which promoted high-intensity local heating and resulted to increased cross-linking during the curing stage [42,43]. Similarly, the degasification process promoted free-radical polymerization and increased cross-linking network. The presence of oxygen in organic precursors usually led to the formation of stable peroxide, which limits the degree of conversion at the initial stages of carbonization [16,44]. The increased cross-linking promoted by these preparation procedures during the curing stage led to significant reduction of the attained graphitization level. However, no significant difference was obtained in their overall carbons' oxidation stability compared to the samples, which have a higher amount of graphite in their composition. The amount of residual mass for Nv-6B-*M*-U and Nv-10H-*M*-U (based on the introduction of additional ultrasonic mixing) was 51% and 53% respectively. Similarly, 49% and 50% residual mass were recorded for Nv-6B-*M*-V and Nv-10H-*M*-V (based additional vacuum degassing after mechanical mixing) carbons respectively. These values are close to those of Nv-6B-M (~50%) and Nv-10H-M (~52%). The likely reason for the similar performance might be the balance between the various factors affecting their oxidation behavior. These observations agree with the submission of Ruff et al. [6] that carbons' oxidation is influenced by several factors, which include the extent and accessibility of its surface, bond strength of its atoms and composition. Consequently, a combination of several characterization techniques may be required to establish a correlation between graphitization and oxidation behavior of these carbons.

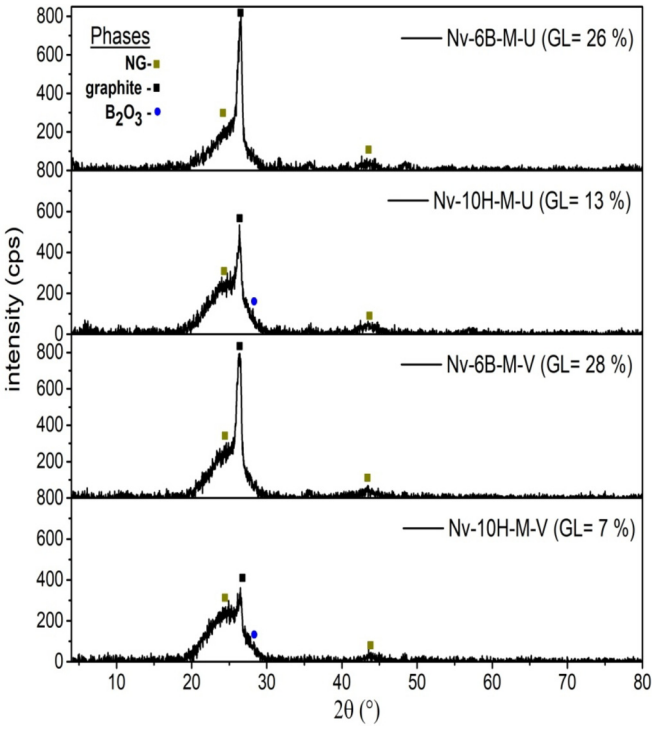

Fig. 8. XRD profiles of the prepared samples showing the effect of additional ultrasonic mixing and vacuum degassing on catalytic graphitization of novolac resin after firing at 1000 °C for 5h under reducing atmosphere. GL = graphitization level, NG = non-graphitic.

4. Conclusion

The structural evolution that occurs when catalyzed novolac resin containing boron oxide or boric acid was subjected to thermal treatment was studied using FTIR technique. The results show that the graphitizing additives were incorporated into the resin structure. The graphitization at a lower temperature (1000 °C) of carbons derived from novolac resin containing boron source additives was attributed to the formation of B–*O*–B bonds as well as formation and cleavage of B–*O*–C bonds during heat treatments. The lower binding energy of B–*O*–C bonds compared to C–C ones promote atoms rotation and rearrangement during the pyrolysis operation that favors graphite generation.

Carbons derived from catalytic graphitization of novolac show improved oxidation resistance than those of the plain resin. However, their thermal stability in the oxidizing environment was found to depend on other factors such as composition. Boron oxide detected in the samples protects the carbons edges and improved their oxidation resistance. Moreover, carbons derived from the boron compounds modified resin containing HMTA also show improved oxidation resistance although graphite was not generated during their pyrolysis. This was attributed to the increased

cross-linking at the curing stage, (due to the presence of hexamethylenetetramine) which impeded graphite generation during pyrolysis but promotes increased carbon atoms bond strength. The same behavior was observed when factors such as ultrasonic mixing and vacuum degassing, which caused increased curing degree were employed during the formulation stage [16]. Based on these findings, it was proposed that carbon atoms' cross-linking strength, atomic arrangement and composition effect are controlling factors affecting the oxidation resistance of carbons derived from the boron compounds modified novolac resin. Therefore, better oxidation resistance may be attained without achieving crystallization of carbons derived from novolac resin. However, the thermomechanical and chemical properties of CCRs depends on the presence of carbons with feature close to graphite. Hence, the benefits derived from producing graphite from novolac resin carbons are not limited to improved oxidation resistance.

Acknowledgements

This project was supported by a Ph.D. research fellowship from TWAS/CNPq. The authors are grateful to RHI-Magnesita for providing some of the raw materials used in this research.

References

[1] H. Jansen, Bonding of MgO-C bricks by catalytically activated resin, Millenn. Steel Int. (2007) 95–98.
[2] W. Schulle, J. Ulbricht, Influence of different carbonaceous binders on the properties of refractories, Boletín de la Sociedad Española de Cerám, Vidrio 31 (1992) 419–525.
[3] C. Schacht, Refractories Handbook, CRC Press, 2004.
[4] A. Gardziella, L.A. Pilato, A. Knop, Phenolic Resins: Chemistry, Applications, Standardization, Safety and Ecology, 2 ed., Springer-Verlag Berlin Heidelberg, New York, 2000.
[5] W. Lian, H. Song, X. Chen, L. Li, J. Huo, M. Zhao, G. Wang, The transformation of acetylene black into onion-like hollow carbon nanoparticles at 1000 °C using an iron catalyst, Carbon 46 (2008) 525–530.
[6] O. Ruff, Reactions of solid carbon with gases and liquids, Trans. Faraday Soc. 34 (1938) 1022–1033.
[7] K.G. Gallagher, G. Yushin, T.F. Fuller, The role of nanostructure in the electrochemical oxidation of model-carbon materials in acidic environments, J. Electrochem. Soc. 157 (2010) 820–830.
[8] W.R. Smith, M.H. Polley, The oxidation of graphitized carbon black, J. Phys. Chem. 60 (1956) 689–691.
[9] S.E. Stein, R.L. Brown, Chemical theory of graphite-like molecules, Carbon 23 (1985) 105–109.
[10] J. Wang, N. Jiang, H. Jiang, Micro-structural evolution of phenol-formaldehyde resin modified by boron carbide at elevated temperatures, Mat. Chem. and Phys. 120 (2010) 187–192.
[11] C.S. Bitencourt, A.P. Luz, C. Pagliosa, V.C. Pandolfelli, Role of catalytic agents and processing parameters in the graphitization process of a carbon-based refractory binder, Ceram. Int. 41 (2015) 13320–13330.
[12] A.P. Luz, C.G. Renda, A.A. Lucas, R. Bertholdo, C.G. Aneziris, V.C. Pandolfelli, Graphitization of phenolic resins for carbon-based refractories, Ceram. Int. 43 (2017) 8171–8182.
[13] F. Liang, N. Li, X.-k. Li, W. Yan, Effect of the addition of carbon black and carbon nanotubes on the structure and oxidation resistance of pyrolyzed phenolic carbons, Carbon 51 (2013) 436.
[14] B. Zhu, G. Wei, X. Li, L. Ma, Y. Wei, Structure evolution and oxidation resistance of pyrolytic carbon derived from FE doped phenol resin, in: Proceedings of the Unified International Technical Conference on Refractories (UNITECR 2013), John Wiley & Sons, Inc, 2014, pp. 1075–1080.
[15] D.H. Grosse, H. Jansen, P. Bartha, Carbonaceous Refractory Shaped Body with Improved Oxidation Behavior and Batch Composition and Method for Producing the Same, 2001. Google Patents.
[16] S.I. Talabi, A.P. Luz, A.A. Lucas, C. Pagliosa, V.C. Pandolfelli, Catalytic graphitization of novolac resin for refractory applications, Ceram. Int. 44 (2018) 3816–3824.
[17] J. Parsons, Vibrational spectra of orthorhombic metaboric acid, J. Chem. Phys. 33 (1960) 1860–1866.
[18] L. Andrews, T.R. Burkholder, Infrared spectra of molecular $B(OH)_3$ and HOBO in solid argon, J. Chem. Phys. 97 (1992) 7203–7210.
[19] E.F. Medvedev, A.S. Komarevskaya, IR spectroscopic study of the phase composition of boric acid as a component of glass batch, Glass Ceram. 64 (2007) 42–46.
[20] A.I. Ermolaeva, N.I. Koshelev, S.A. Dvornikov, Investigation of borophosphosilicate glasses synthesized by the sol-gel method, Glass Phys. Chem. 26 (2000) 300–302.
[21] A.S.M. Menachem Lewin, E. Pearce, Flame-retardant Polym. Mat., Springer, US, 2012.
[22] R.T. Conley, J.F. Bieron, A study of the oxidative degradation of phenol-formaldehyde polycondensates using infrared spectroscopy, J. Appl. Polym. Sci. 7 (1963) 103–117.
[23] R. Lee, Phenolic Resin Chemistry and Proposed Mechanism for Thermal Decomposition, NASA Marshall Space Flight Center, Washington, 2007, pp. 7–13.
[24] Y. Liu, J. Gao, R. Zhang, Thermal properties and stability of boron-containing phenol-formaldehyde resin formed from paraformaldehyde, Polym. Degrad. Stabil. 77 (2002) 495–501.
[25] M.K. Ida Poljanšek, Characterization of phenol-formaldehyde prepolymer resins by in-line FT-IR spectroscopy, Acta Chim. Slov. 52 (2005) 238–244.
[26] S. Theodoropoulou, D. Papadimitriou, L. Zoumpoulakis, J. Simitzis, Structural and optical characterization of pyrolytic carbon derived from novolac resin, Anal. Bioanal. Chem. 379 (2004) 788–791.
[27] A. Ertugrul, M.H. Alma, O. Gonultas, Z. Candan, M. Ertas, FTIR investigation of phenol formaldehyde resin modified with boric acid, in: V.L. Herian (Ed.), Proceedings of the 55th International Convention of Society of Wood Science and Technology, China, 2012, pp. 480–487.
[28] S. Wang, Y. Wang, C. Bian, Y. Zhong, X. Jing, The thermal stability and pyrolysis mechanism of boron-containing phenolic resins: the effect of phenyl borates on the char formation, Appl. Surf. Sci. 331 (2015) 519–529.
[29] A.M. Kawamoto, L.C. Pardini, M.F. Diniz, V.L. Lourenço, M.F.K. Takahashi, Synthesis of a boron-modified phenolic resin, J. Aerosp.Technol. Manag. 2 (2010) 169–182.
[30] S. Wang, X. Jing, Y. Wang, J. Si, Synthesis and characterization of novel phenolic resins containing aryl-boron backbone and their utilization in polymeric composites with improved thermal and mechanical properties, Polym. Adv. Technol. 25 (2014) 152–159.
[31] W.-F. Zhang, C.-L. Liu, Y.-G. Ying, W.-S. Dong, The preparation and characterization of boron-containing phenolic fibers, Mater. Chem. Phys. 121 (2010) 89–94.
[32] J. Simitzis, L. Zoumpoulakis, Influence of FeCl3 dopant on the electrical conductivity of pyrolysed aromatic polymers, J. Mater. Sci. 31 (1996) 1615–1620.
[33] T. Enoki, M. Suzuki, M. Endo, Graphite Intercalation Compounds and Applications, Oxford University Press, 2003.
[34] D.-E. Jiang, A.C.T. van Duin, W.A. Goddard, S. Dai, Simulating the initial stage of phenolic resin carbonization via the ReaxFF reactive force field, The J. of Phys.l Chem. A 113 (2009) 6891–6894.
[35] D. Ila, G.M. Jenkins, L.R. Holland, L. Evelyn, H. Jena, A study of the thermally induced carbonization of phenol-formaldehyde by combined ion beam and surface specific analyses, Vacuum 45 (1994) 451–454.
[36] S.J. Šupová Monika, C. Zdeněk, Č. Martin, W. Zuzana, S. Tomáš, M. Vladimír, S. Zbyněk, Ž. Margit, Relation between mechanical properties and pyrolysis temperature of phenol formaldehyde resin for gas separation membranes, Ceram.-Silikáty 56 (2012) 40–49.
[37] G. Savage, Thermosetting Resin Matrix Precursors, Carbon-carbon Comp, Springer Netherlands, Dordrecht, 1993, pp. 117–156.
[38] P. Xu, X. Jing, High carbon yield thermoset resin based on phenolic resin, hyperbranched polyborate, and paraformaldehyde, Polym. Adv. Technol. 22 (2011) 2592–2595.
[39] I.A.S. Edwards, H. Marsh, Introduction to Carbon Science, Butterworths, 1989.
[40] A. Gardziella, J. Suren, M. Belsue, Carbon from Phenolic Resins : Carbon Yield and Volatile Components. Recent Studies, Expert Fachmedien GmbH, Allemagne, 1992.
[41] D. Mang, H.P. Boehm, K. Stanczyk, H. Marsh, Inhibiting effect of incorporated nitrogen on the oxidation of microcrystalline carbons, Carbon 30 (1992) 391–398.
[42] S.-G. Zhao, B.-C. Wang, Q. Sun, Effect of physical disturbance on the structure of needle coke, Chin. Phys. B 19 (2010) 108101.
[43] K.S. Suslick, W.L. Nyborg, Ultrasound: its chemical, physical and biological effects, J. Acoust. Soc. Am. 87 (1990) 919–920.
[44] M. Pilkenton, J. Lewman, R. Chartoff, Effect of oxygen on the crosslinking and mechanical properties of a thermoset formed by free-radical photocuring, J. Appl. Polym. Sci. 119 (2011) 2359–2370.